

Density-Functional Calculations of the Normal Vibrations for the Triplet Excited State of C₆₀

Toshiki Hara, Jun Onoe and Kazuo Takeuchi

RIKEN (The Institute of Physical and Chemical Research), 2-1 Hirosawa, Wako, Saitama 351-0198, Japan
Fax: 81-48-462-4702, e-mail: thara@postman.riken.go.jp

The geometries and normal vibrations for the ground (S_0) and lowest triplet excited (T_1) states of the C₆₀ molecule were investigated using density-functional calculations. It was found that the most stable symmetry for the T_1 state is D_{5d} , and its Jahn-Teller distortion mainly arises from the h_g (268 cm^{-1}) vibrational mode. The calculated frequency and intensity of the IR active modes for the T_1 state were both different from those for the S_0 state. A significant difference in the potential energy surface between the S_0 and T_1 states was found.

Key words: C₆₀, triplet excited state, vibrational frequencies, Jahn-Teller effect, Duschinsky effect

1. INTRODUCTION

After the photo-excitation of C₆₀ from its ground state (S_0) to the singlet excited states (S_n), the internal conversion to the lowest singlet excited state (S_1) and subsequent intersystem crossing to the lowest triplet excited state (T_1) rapidly take place.¹⁾ Because the quantum efficiency of the $S_1 \rightarrow T_1$ transition is close to unity¹⁾ and the lifetime of the triplet state T_1 is very long ($40\text{ ms}^{1)}$ compared with that of the singlet state S_1 ($1.2\text{ ns}^{2)}$), the triplet state T_1 plays an important role in the photo-induced reaction of C₆₀ such as cycloadditional dimerization³⁾, singlet oxygen production, etc. Accordingly, the information on the potential energy surface of the triplet state T_1 is important to understand the mechanism of the photo-induced reaction of C₆₀.

It is well known that the I_h symmetry in the ground state S_0 does not hold in the triplet T_1 state and is lowered by the Jahn-Teller effect.⁴⁾ Theoretical calculations based on the semi-empirical model predicted that the most stable geometry of the T_1 state has D_{5d} symmetry.⁴⁾⁻⁷⁾ However, the energy difference between the most stable D_{5d} geometry and second (D_{2h}) or third (D_{3d}) stable ones is very small (65 mV for the former and 126 meV for the latter⁷⁾). This suggests that the most stable symmetry of the T_1 state is difficult to experimentally determine. The experiments to investigate the symmetry for the T_1 state of C₆₀ have been carried out in the crystalline or in an inert-gas matrix using electron spin resonance (ESR)⁸⁾ and optically detected magnetic resonance (ODMR)⁹⁾. Although most studies assigned the symmetry of the T_1 state as D_{5d} ,⁸⁾ there still remains another possibility to assign it as D_{2h} by reflecting the theoretical prediction. This problem prompts us to perform the geometry optimization of the triplet T_1 state with a more sophisticated treatment.

In the present work, we determined the most

stable geometry of the T_1 state using density-functional theory and obtained the frequencies and normal coordinates in order to clarify the potential energy surface of the T_1 state.

2. COMPUTATIONAL METHOD

The geometry optimization for the S_0 and T_1 states of C₆₀ was performed on the basis of the density-functional theory (DFT) using the Amsterdam density functional (ADF) program developed by Baerends *et al.*¹⁰⁾⁻¹³⁾ In the geometry optimization of the T_1 state, the potential minimum was searched in the D_{5d} , D_{3d} and D_{2h} symmetries as the most likely candidates.⁵⁾⁻⁷⁾ The frequency calculations were done for the optimized S_0 and T_1 geometries. The local exchange-correlation functional given by Vosko, Wilk and Nusair (VWN) was used in the Hamiltonian of the electronic systems.¹⁴⁾ The Kohn-Sham molecular orbitals were expanded by the double- ζ Slater-type basis set of the carbon $2s$ and $2p$ orbitals along with the $3d$ polarization functions. The $1s$ orbital was treated by the frozen-core approximation. The electronic configuration of the T_1 state was expressed by a single-electron excitation from the highest occupied molecular orbital (HOMO) to the lowest unoccupied molecular orbital (LUMO) in the ground state S_0 . All the calculations were carried out with a workstation (V-T Alpha 533, Visual Technology).

3 RESULTS AND DISCUSSION

3.1 Geometry

The results of the geometry optimization for the S_0 and T_1 states are summarized in Table I. Where, $d(\text{C}-\text{C})$ denotes the "single-bond length" of C₆₀ defined by a bond length owned by a five-membered carbon ring and an adjacent six-membered carbon ring of C₆₀. Likewise, $d(\text{C}=\text{C})$ denotes the "double-bond length" of C₆₀ defined by a bond length owned by two adjacent six-membered carbon-rings of C₆₀.

Table I The bonding energy E_B (eV), single-bond length $d(C-C)$ (Å), double-bond length $d(C=C)$ (Å) and radius R (Å) of the optimized ground S_0 and triplet T_1 states of C_{60} .

State	E_B	$d_{\min}(C-C)$ $d_{\max}(C-C)$	$d_{\min}(C=C)$ $d_{\max}(C=C)$	R_{\min} R_{\max}
$S_0(I_h)$	-578.307	1.436	1.384	3.511
$T_1(D_{5d})$	-576.837	1.412 1.443	1.379 1.403	3.497 3.541
$T_1(D_{3d})$	-576.785	1.423 1.445	1.383 1.404	3.494 3.532
$T_1(D_{2h})$	-576.771	1.422 1.446	1.383 1.400	3.498 3.538

R denotes the "radius" of C_{60} defined by a length between the center of C_{60} and one of the carbon atoms.

The bonding energy (E_B) of the ground state S_0 was -578.307 eV, while that for the most stable D_{5d} geometry of the T_1 state was -576.837 eV. The energy difference (1.470 eV) between the S_0 and T_1 states is in good agreement with the experimental value of 1.584 eV obtained by laser-induced phosphorescence spectroscopy.¹⁵⁾ The E_B of the D_{3d} (-576.785 eV) and D_{2h} (-576.771 eV) geometries were slightly larger by 52 and 66 meV than that of the D_{5d} geometry, respectively.

There are 60 single-bonds and 30 double-bonds in C_{60} . Due to the highest symmetry of the molecule in the S_0 state, the values of $d(C-C)$, $d(C=C)$ and R are uniquely given. The values of 1.436 Å for $d(C-C)$ and 1.384 Å for $d(C=C)$ in Table I are in good agreement with the experimental values of 1.436 Å and 1.398 Å obtained by electron diffraction¹⁶⁾, respectively. This agreement allows us to discuss the geometry of the triplet T_1 state.

Due to the symmetry lowering in the triplet T_1 state, $d(C-C)$ has four, six, and nine different values for the D_{5d} , D_{3d} , and D_{2h} symmetry, respectively. On the other hand, $d(C=C)$ has three, four, and six different values for the D_{5d} , D_{3d} , and D_{2h} symmetry, respectively. For similar reason, R has four, six, and nine different values for the D_{5d} , D_{3d} , and D_{2h} symmetry, respectively. Table I shows the maximum and minimum values of the $d(C-C)$, $d(C=C)$, and R for the three T_1 states. It is found that the Jahn-Teller distortion of the triplet T_1 state is not large. For example, the difference between the R_{\min} and R_{\max} of the D_{5d} symmetry is only 0.044 Å. Figure 1 shows the atomic displacement vectors in going from the ground state S_0 to the triplet excited state T_1 with the D_{5d} symmetry. The left-hand side of Fig. 1 shows the view along the C_5 principal axis of the point group. Similarly, the right-hand side shows the view perpendicular to the principal axis. The solid and dotted lines in the T_1 frame-

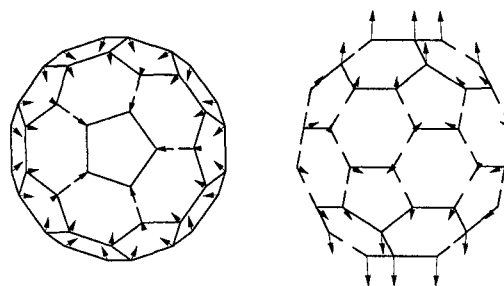


Fig.1 The atomic displacement vectors from the ground state S_0 to the triplet state T_1 with the D_{5d} symmetry.

Table II Weight (W_{JT}) of the normalized S_0 - T_1 atomic displacement vectors in the normal coordinates of the total symmetric a_g modes and Jahn-Teller active h_g modes of S_0 .

mode	cm^{-1}	W_{JT}
$a_g(1)$	502	0.00
$a_g(2)$	1531	0.01
$h_g(1)$	269	0.86
$h_g(2)$	430	0.00
$h_g(3)$	711	0.01
$h_g(4)$	794	0.04
$h_g(5)$	1129	0.00
$h_g(6)$	1288	0.01
$h_g(7)$	1475	0.03
$h_g(8)$	1609	0.02

work indicate the shrunk and elongated C-C bonding compared with that of S_0 , respectively. The length of the displacement vectors is proportional to the magnitude of the real atomic displacement. For the molecular distortion from the S_0 to the T_1 state, the molecule elongates along the principal axis and shrinks toward the axis.

3.2 Normal vibrations

The normal vibrations of the ground S_0 and the triplet T_1 states are now discussed. The C_{60} molecule has 46 different frequencies in the 174 independent normal vibrations for the ground state S_0 with symmetry I_h . They are assigned as $2a_g + 3t_{1g} + 4t_{2g} + 6g_g + 8h_g + a_u + 4t_{1u} + 5t_{2u} + 6g_u + 7h_u$, where the a type mode is non-degenerate, and the t , g and h type modes are three-, four- and five-fold degenerate, respectively. The distortion of the triplet state T_1 arises along the normal coordinates of the total symmetric a_g modes and Jahn-Teller active h_g modes of S_0 .⁴⁾ In order to examine the contribution of a_g and h_g modes to the distortion of the T_1 state with the D_{5d} symmetry, we normalized the S_0 - T_1 atomic displacement vectors and expanded

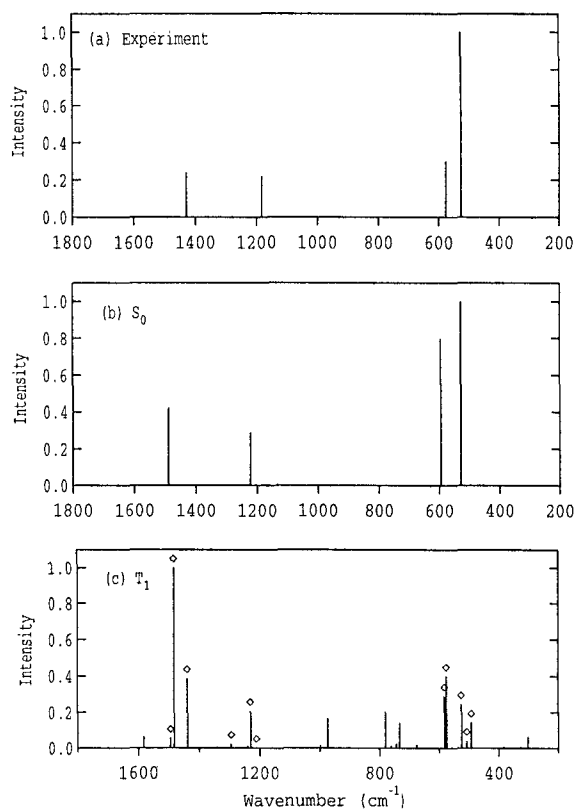


Fig.2 (a) Observed and (b) calculated IR frequencies and normalized intensities of the S_0 state. (c) Calculated IR frequencies and normalized intensities of the T_1 state.

them into the normal coordinates of these modes. Table II shows the squared expansion coefficients W_{JT} . It is found that the dominant contribution to the Jahn-Teller distortion arises from the lowest h_g vibration (269 cm^{-1}).

For the ground state S_0 , only four t_{1u} vibrations are IR active. Figures 2(a) and 2(b) compare the experimentally obtained¹⁷⁾ frequencies and intensities of the IR active modes with those calculated. The calculated frequencies and intensities satisfactorily agree with the experiment. As the molecular symmetry is lowered from the I_h in the S_0 state to D_{5d} in the T_1 state, the irreducible representation of the I_h is reduced to those of the D_{5d} . For example, the *gerade* representation of the I_h is reduced as $A_g \rightarrow A_{1g}$, $T_{1g} \rightarrow E_{1g} + A_{2g}$, $T_{2g} \rightarrow E_{2g} + A_{2g}$, $G_g \rightarrow E_{1g} + E_{2g}$, and $H_g \rightarrow A_{1g} + E_{1g} + E_{2g}$. Similar reduction occurs in the *ungerade* representation. There are 104 different frequencies in the 174 independent normal vibrations for the T_1 state with the D_{5d} symmetry. They are assigned as $10a_{1g} + 7a_{2g} + 17e_{1g} + 18e_{2g} + 8a_{1u} + 9a_{2u} + 17e_{1u} + 18e_{2u}$, where the e type mode is two-fold degenerate. Among them,

the a_{2u} and e_{1u} modes are IR active. Figure 2(c) shows the calculated frequencies and IR intensities for the T_1 state. Although Table I shows that the geometry of the T_1 state is not very different from that of the S_0 state, the IR spectra are quite different as shown in Fig. 2. For example, the relative intensity between the regions of $400\text{--}500\text{ cm}^{-1}$ and $1100\text{--}1500\text{ cm}^{-1}$ for the S_0 state is opposite to that for the T_1 state.

The Born-Oppenheimer potential energy surface of the T_1 state is now discussed using the calculated frequencies and normal coordinates. The difference in the potential energy surface between the S_0 and T_1 states is characterized by their curvatures at the energy minimum and their relative position in the normal coordinate space. The latter case, which is known as the Duschinsky effect¹⁸⁾; the rotations of the normal coordinates of excited states relative to those of the ground state, is usually neglected but sometimes important when considering the vibronic structures in which the absorption and luminescence spectra are not the mirror image of each other.^{19)–21)}

We examined the Duschinsky effect of the T_1 state by expansion of the normal coordinates of the T_1 state into those of the S_0 state. Table III shows the calculated (squared) expansion coefficients (W_D) for the total symmetric a_{1g} modes. It is found that the lowest $a_{1g}(1)$ mode of T_1 consists mostly (96%) of the lowest $h_g(1)$ mode of S_0 . This indicates that the potential curve along the $a_{1g}(1)$ axis of T_1 is almost parallel with that of the $h_g(1)$ axis of S_0 . Furthermore, the frequency shift from 269 cm^{-1} of $h_g(1)$ to 243 cm^{-1} of $a_{1g}(1)$ indicates that the potential well along the $a_{1g}(1)$ axis of T_1 widens compared with that along the $h_g(1)$ axis of S_0 . On the other hand, the second lowest mode $a_{1g}(2)$ consists of 54% $a_g(1)$ and 42% $h_g(2)$ modes of S_0 . The third lowest mode $a_{1g}(3)$ consists of 44% $a_g(1)$ and 54% $h_g(2)$ modes of S_0 . The opposite composition between the $a_{1g}(2)$ and $a_{1g}(3)$ modes is because the rectangular $a_{1g}(2)$ – $a_{1g}(3)$ coordinate of T_1 rotates against the rectangular $a_g(1)$ – $h_g(2)$ coordinate of S_0 . The other a_{1g} modes, $a_{1g}(4)$ – $a_{1g}(10)$, for the T_1 state consist of one of the a_g or h_g modes of S_0 without strong mixing.

We also calculated the mixing weight W_D for the IR active a_{2u} and e_{1u} modes of the triplet state T_1 . It was found that the Duschinsky effects become significant for the $a_{2u}(6)$ and $a_{2u}(7)$ modes and for the $e_{1u}(3)$, $e_{1u}(4)$, $e_{1u}(13)$, $e_{1u}(14)$, $e_{1u}(15)$, $e_{1u}(16)$ and $e_{1u}(17)$ modes. Especially, the $e_{1u}(16)$ modes of the T_1 state consisted of three modes, $g_u(6)$, $t_{1u}(4)$ and $h_u(7)$, of the S_0 state. These results give us some information on the changes in the potential surfaces of the IR active modes between the S_0 and T_1 states. As described above, the three-fold t_{1u} modes of S_0 split into the a_{2u} and two-fold e_{1u} modes for the D_{5d} symmetry. Indeed, the $t_{1u}(2)$ mode splits into the $a_{2u}(3)$ and two-fold $e_{1u}(5)$ modes. However, other modes, $t_{1u}(1)$, $t_{1u}(3)$

Table III The mixing weight (W_D) of the vibrational coordinates of the S_0 state in the a_{1g} modes of the T_1 state.

T_1	cm^{-1}	S_0	cm^{-1}	W_D
$a_{1g}(1)$	234	$h_g(1)$	269	0.96
$a_{1g}(2)$	376	$a_g(1)$	502	0.54
		$h_g(2)$	430	0.42
$a_{1g}(3)$	449	$h_g(2)$	430	0.54
		$a_g(1)$	502	0.44
$a_{1g}(4)$	737	$h_g(3)$	711	0.95
$a_{1g}(5)$	776	$h_g(4)$	794	0.96
$a_{1g}(6)$	1140	$h_g(5)$	1129	0.99
$a_{1g}(7)$	1286	$h_g(6)$	1288	1.00
$a_{1g}(8)$	1482	$h_g(7)$	1475	0.99
$a_{1g}(9)$	1526	$a_g(2)$	1531	0.98
$a_{1g}(10)$	1617	$h_g(8)$	1609	0.98

and $t_{1u}(4)$, do not exhibit this tendency. Actually, the $t_{1u}(1)$ mode triply splits into the $a_{2u}(2)$, $e_{1u}(3)$ and $e_{1u}(4)$ modes of the T_1 state. This further splitting of the e_{1u} modes is due to the mixing of the silent $h_u(2)$ mode of the S_0 state. The $t_{1u}(3)$ mode also splits into the $a_{2u}(6)$, $a_{2u}(7)$ and $e_{1u}(11)$ modes as a result of the mixing of the $t_{2u}(4)$ mode. In similar manner, the $t_{1u}(4)$ mode splits into $a_{2u}(8)$, $e_{1u}(15)$ and $e_{1u}(16)$ modes by the mixing of the $g_u(6)$ mode. From these results, the absorption due to the $t_{1u}(2)$ mode in the IR spectrum of the S_0 state may doubly split in the T_1 state. However, the absorption of the $t_{1u}(1)$, $t_{1u}(3)$ and $t_{1u}(4)$ modes each triply split. In Figure 2(c), the IR intensity originating from the four t_{1u} modes for the S_0 state is marked by "◇". This splitting pattern in the IR absorption of the t_{1u} modes plays an important role in determining the symmetry of the T_1 state.

4 CONCLUSIONS

The geometries and vibrational frequencies for the ground state S_0 and lowest excited triplet state T_1 of the C_{60} molecule have been calculated using DFT. The most stable geometry of the T_1 state is found to be the D_{5d} symmetry. However, the energy splitting between the D_{5d} and D_{3d} (52 meV) or D_{2h} (66 meV) is small. Although the Jahn-Teller distortion of the T_1 state is small, the calculated IR stick spectrum of the state is different from that of the S_0 state. The potential energy surface of the T_1 state was examined from the viewpoint of its shape and position in the normal coordinate space. It was found that the Duschinsky effect becomes significant in some vibrational modes of the T_1 state.

ACKNOWLEDGEMENTS

This work was supported in part by special coordination funds from the Science and Technology Agency of the Japanese Government. One of the authors (T.H.) thanks the Special Postdoctoral Researchers Program of RIKEN.

REFERENCES

- [1] J. W. Arbogast, A. P. Darmany, C. S. Foote, Y. Rubin, F. N. Diederich, M. M. Alvarez, S. J. Anz, and R. L. Whetten, *J. Phys. Chem.*, **95**, 11-12 (1991).
- [2] T. W. Ebbesen, K. Tanigaki, and S. Kuroshima, *Chem. Phys. Lett.*, **181**, 501-504 (1991).
- [3] A. M. Rao, P. Zhou, K. -A. Wang, G. T. Hager, J. M. Holden, Y. Wang, W. -T. Lee, X. -X. Bi, P. C. Eklund, D. S. Cornett, M. A. Duncan, and I. J. Amster, *Science* **259** 955-957 (1993).
- [4] F. Negri, G. Orlandi, and F. Zerbetto, *Chem. Phys. Lett.*, **144**, 31-37 (1988).
- [5] P. R. Surján, L. Udvardi, and K. Németh, *J. Mol. Struct. (Theochem)*, **311**, 55-68 (1994).
- [6] P. R. Surján, K. Németh, M. Bennati, A. Grupp, and M. Mehring, *Chem. Phys. Lett.*, **251**, 115-118 (1996).
- [7] M. Kállay, K. Németh, and P. R. Surján, *J. Phys. Chem.*, **102**, 1261-1273 (1998).
- [8] N. Mizuochi, Y. Ohba, and S. Yamaguchi, *J. Phys. Chem.*, **111**, 3479-3487 (1999), and references therein.
- [9] A. Angerhofer, J. U. von Schütz, D. Widmann, W. H. Müller, H. U. ter Mers, and H. Sixl, *Chem. Phys. Lett.*, **217**, 403-408 (1994).
- [10] ADF 2.3.0, Theoretical Chemistry, Vrije Universiteit, Amsterdam
- [11] E. J. Baerends, D. E. Ellis, and P. Ros, *Chem. Phys.*, **2**, 41-51 (1973).
- [12] G. te Velde and E. J. Baerends, *J. Comp. Phys.*, **99**, 84-98 (1992).
- [13] C. F. Guerra et al. METECC-95 (1995) 305
- [14] S. H. Vosko, L. Wilk, and M. Nusair, *Can. J. Phys.*, **58**, 1200-1211 (1980).
- [15] W.-C. Hung, C.-D. Ho, C.-P. Liu, and Y.-P. Lee, *J. Phys. Chem.*, **100**, 3927-3932 (1996).
- [16] K. Hedberg, L. Hedberg, D. S. Bethune, C. A. Brown, H. C. Dorn, R. D. Johnson, and M. de Vries, *Science* **254** 410-412 (1991).
- [17] J. Onoe and K. Takeuchi, *Phys. Rev. B* **54** 6167-6171 (1996).
- [18] F. Duschinsky, *Acta Physicochim. U.S.S.R.*, **7**, 551-566 (1937).
- [19] B. Sharf and B. Honig, *Chem. Phys. Lett.*, **7**, 132-136 (1970).
- [20] G. J. Small, *J. Chem. Phys.*, **54**, 3300-3306 (1971).
- [21] A. Peluso, F. Santoro, and G. D. Re, *Int. J. Quantum Chem.*, **63**, 233-244 (1996).

(Received December 17, 1999; Accepted March 18, 2000)